Supporting Information

Fluorination of Boron-doped Diamond Film Electrodes for Minimization of Perchlorate Formation

Pralay Gayen[a] and Brian P. Chaplin[a,] *

[a]*Department of Chemical Engineering, University of Illinois at Chicago, Chicago, IL 60607, USA*

* Corresponding author: Phone No.: +13129960288, E-mail: chaplin@uic.edu (Brian P. Chaplin)

1. Mass Transfer Coefficient.

The Levich equation (S1) was used to calculate the mass transfer coefficient for the i^{th} species $(k_{m,i})$[1], and was used to calculate the mass transfer rate (r_i) (equation S2).

$$k_{m,i} = 0.62\, D_i^{2/3} \omega^{1/2} \nu^{-1/6} \quad \text{(S1)}$$

$$r_i = k_{m,i} C_i \quad \text{(S2)}$$

where D_i is the diffusion coefficient for the i^{th} compound, ω is the rotation speed per sec., ν is the kinematic viscosity of water (1.0 x 10^{-6} m^2 s^{-1}), and C_i is the initial bulk concentration of the i^{th} species. Diffusion coefficients for phenol and terephthalic acid (TA) were 9×10^{-10} m^2 s^{-1} and 4×10^{-10} m^2 s^{-1}, respectively[2,3]. The electrode rotation rate was 523.6 s^{-1} (5000 rpm). The mass transfer rates of phenol (1mM) and TA (0.1mM) were calculated as 7.99 mmole m^{-2} min^{-1} and 0.463 mmole m^{-2} min^{-1}, respectively.

2. XPS Characterization.

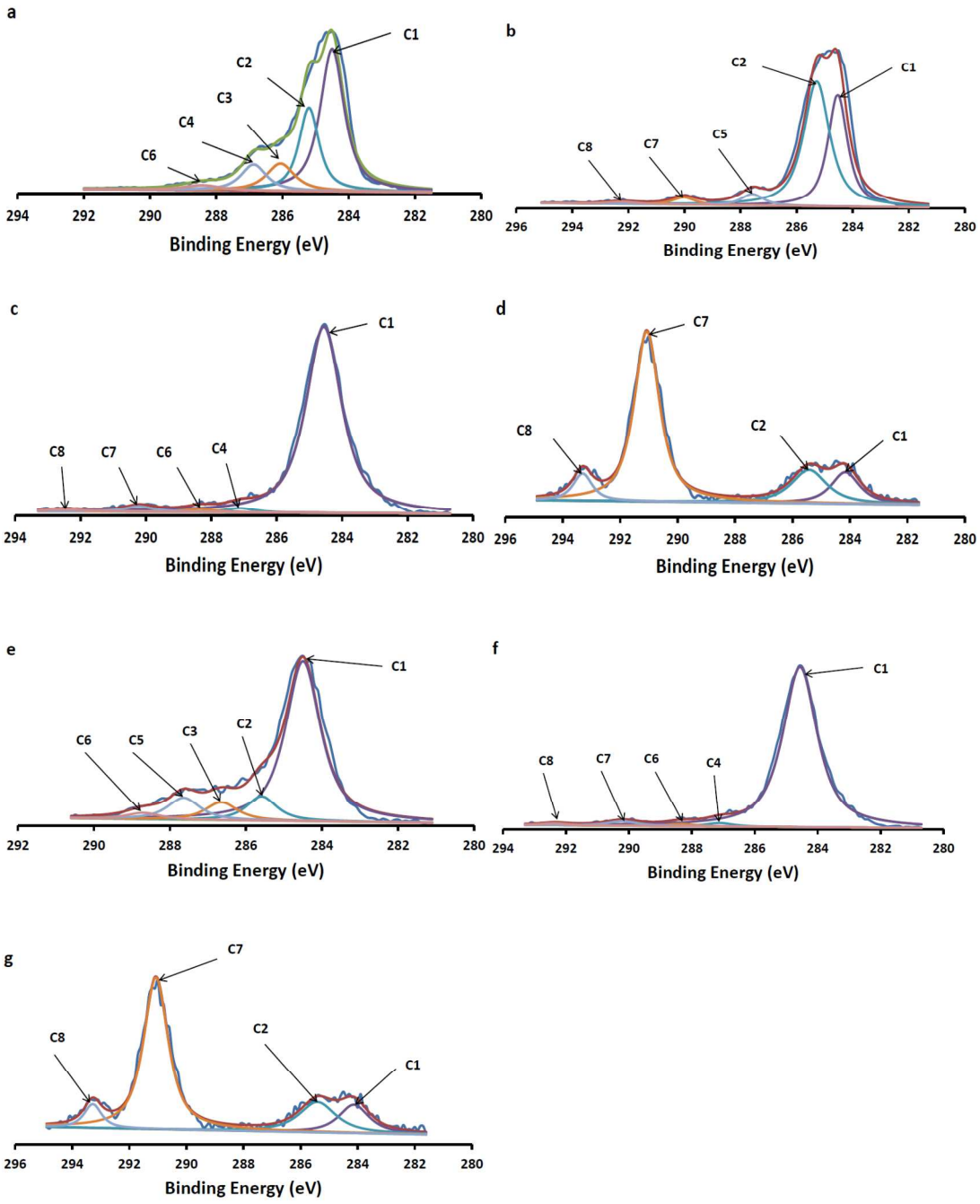

Figure S1. Deconvoluted results of C 1s XPS spectra of a) BDD-O, b) BDDF-plasma, c) BDDF-PFOA, d) BDDF-aliphatic, e) BDDF-aromatic, f) BDDF-PFOA-aged and g) BDDF-aliphatic-aged. Legend: C1: =C=C=; C2: ≡C-C≡; C3: ≡C-OH; C4: =C=O; C5: ≡C-F; C6: -COOH; C7: $=CF_2$; C8: $-CF_3$

Table S1. Comparison of Atomic Ratios (F:Si, F:C and Si:CF_2:CF_3) of an Aliphatic Silane molecule with BDDF-aliphatic (from XPS) and BDDF-aliphatic-aged (from XPS) and Si:CF of an Aromatic Silane molecule with BDDF-aromatic (from XPS).

Atomic Ratio →	**F:Si**	**F:C**	**Si:CF_2:CF_3**	**Si:CF**
Aliphatic Molecule	17	1.7	1:7:1	-
BDDF-aliphatic	15.6	1.88	0.51:8.3:1	-
BDDF-aliphatic-aged	14.7	1.78	0.54:8.63:1	-
Aromatic Molecule	-	-	-	1:5
BDDF-aromatic	-	-	-	1:4.8

3. Electrochemical Characterization.

The electrochemical response changed after plasma treatment of the BDD electrode. The CV scans (scan rate = 100 mV s^{-1}) in the presence of $Fe(CN)_6^{3-/4-}$ showed a decrease in peak currents for oxidation ($I_{peak,anodic,BDD-O}$= 593 μA to $I_{peak,anodic,BDDF-plasma}$= 255 μA) (Table S2). The plasma treatment also increased the anodic to cathodic peak separation (ΔE_i) from ΔE_{BDD-O} = 212 mV for the BDD-O electrode to $\Delta E_{BDDF-plasma}$ = 1032 mV for the BDDF-plasma electrode (Figure S2a). CV scans in the presence of $Fe^{2+/3+}$ showed an increase in current response ($I_{peak,anodic,BDD-O}$ = 350 μA and $I_{peak,anodic,BDDF-plasma}$= 390 μA) and a decrease in peak separation (ΔE_{BDD-O} = 357 mV and $\Delta E_{BDDF-plasma}$= 182 mV) for BDDF-plasma compared to BDD-O (Table S2 and Figure S2b).

The PFOA modified electrodes and aliphatic silanized BDD electrodes were characterized using the same redox couples. The CV scans (scan rate = 100 mV s^{-1}) in the presence of $Fe(CN)_6^{3-/4-}$ showed a decrease in peak current ($I_{peak,anodic,BDD-O}$= 521 μA and $I_{peak,anodic,BDDF-PFOA}$= 328 μA) and an increased peak separation after fluorination (ΔE_{BDD-O} = 309 mV and $\Delta E_{BDDF-PFOA}$ = 941 mV) (Table S2 and Figure S2c). CV scans in the presence of $Fe^{2+/3+}$ showed a decrease in peak current ($I_{peak,anodic,BDD-O}$= 507 μA and $I_{peak,anodic,BDDF-PFOA}$= 290 μA) and an increase in peak separation (ΔE_{BDD-O}= 225 mV and $\Delta E_{BDDF-PFOA}$= 1110 mV) after fluorination, as shown in Table S2 and Figure S2d.

The CV scans on the BDDF-aromatic electrode with the redox couples ($Fe(CN)_6^{3-/4-}$ and $Fe^{3+/2+}$) showed a similar behavior to the BDDF-PFOA electrode (Figure S2e,f and Table S2). The CV scans in the presence of $Fe(CN)_6^{3-/4-}$ showed a decrease in peak current ($I_{peak,anodic,BDD-O}$= 517 μA and $I_{peak,anodic,BDDF-aromatic}$= 299 μA) and an increase in peak separation ((ΔE_{BDD-O}= 217 mV and ($\Delta E_{BDDF-aromatic}$= 971 mV) after fluorination, as shown in Table S2 and Figure S2e. CV scans in the presence of $Fe^{2+/3+}$ showed a decrease in the peak current ($I_{peak,anodic,BDD-O}$= 510 μA

and $I_{peak,anodic,BDDF\text{-}aromatic}$= 324 μA) and an increase in peak separation ($\Delta E_{BDD\text{-}O}$= 213 mV and $\Delta E_{BDDF\text{-}aromatic}$= 997 mV) after fluorination, as shown in Table S2 and Figure S2f.

The CV scans were also performed on the BDDF-aliphatic electrode to show the effect of silanization on the electron transfer rates. The CV scans (scan rate = 100mV s^{-1}) in the presence of $Fe(CN)_6^{3-/4-}$ did not show any peaks associated with redox reactions (Table S2 and Figure 2a). However, after ageing small peaks were observed (Figure 2c,d).

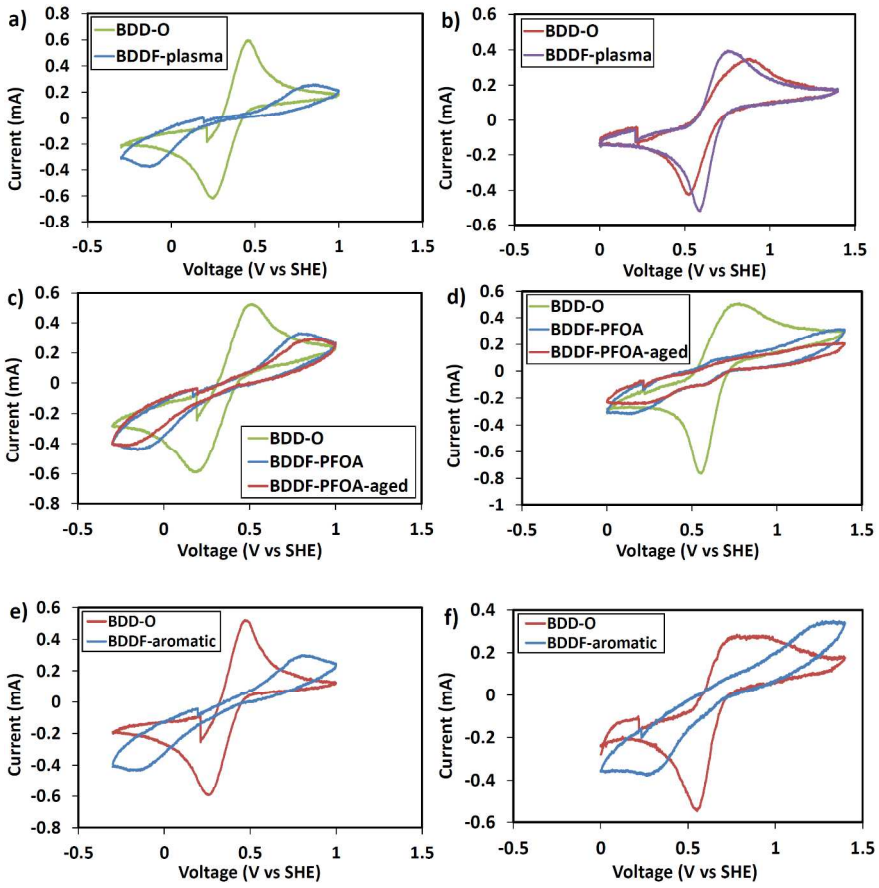

Figure S2 CV scans of: a) BDD-O and BDDF-plasma: 5 mM $Fe(CN)_6^{3-/4-}$; b) BDD-O and BDDF-plasma: 5 mM $Fe^{3+/2+}$; c) BDDF-PFOA and BDDF-PFOA-aged: 5mM $Fe(CN)_6^{3-/4-}$; d) BDDF-PFOA and BDDF-PFOA-aged: 5mM $Fe^{3+/2+}$; e) BDD-O and BDDF-aromatic: 5mM $Fe(CN)_6^{3-/4-}$; f) BDD-O and BDDF-aromatic: 5mM $Fe^{3+/2+}$.

Table S2. CV data of BDD-O, BDDF-plasma, BDDF-PFOA, BDDF-aliphatic, BDDF-aromatic, BDDF-aliphatic-aged and BDDF-PFOA-aged with $Fe(CN)_6^{3-/4-}$ and $Fe^{2+/3+}$ redox couple.

Electrode	$I_{peak,anodic}$ (μA) ($Fe(CN)_6^{3-/4-}$)	$I_{peak,anodic}$ (μA) ($Fe^{2+/3+}$)	ΔE (mV) ($Fe(CN)_6^{3-/4-}$)	ΔE (mV) ($Fe^{2+/3+}$)
BDD-O1*	593	350	212	357
BDDF-plasma	255	390	1032	182
BDD-O2*	521	507	309	225
BDDF-PFOA	328	290	941	1110
BDDF-PFOA-aged	291	202	1041	1052
BDD-O3*	533	316	195	223
BDDF-aliphatic	00	00	-	-
BDDF-aliphatic-aged	58	30	951	1060
BDD-O4*	517	510	217	213
BDDF-aromatic	299	324	971	997

*BDD-O1 = BDD-O before plasma, BDD-O2 = BDD-O before PFOA treatment, BDD-O3 = BDD-O before aliphatic silane treatment and BDD-O4 = BDD-O before aromatic silane treatment

4. Density Functional Theory Optimized Structures

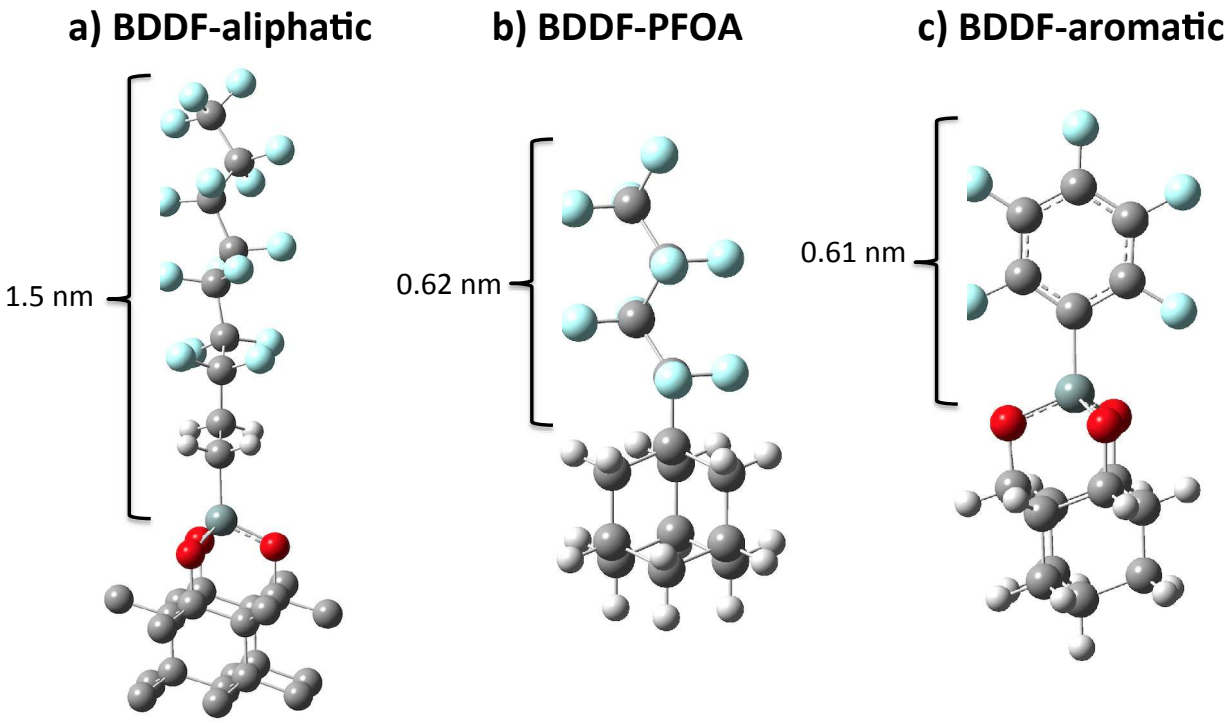

Figure S3. DFT optimized structures of different fluorinated groups for a) BDDF-aliphatic, b) BDDF-PFOA and c) BDDF-aromatic on a 10 carbon atom cluster that represents the BDD surface. Atom key: C (grey); F (teal); O (red); H (white); Si (blue-grey)

5. Additional Experimental Results

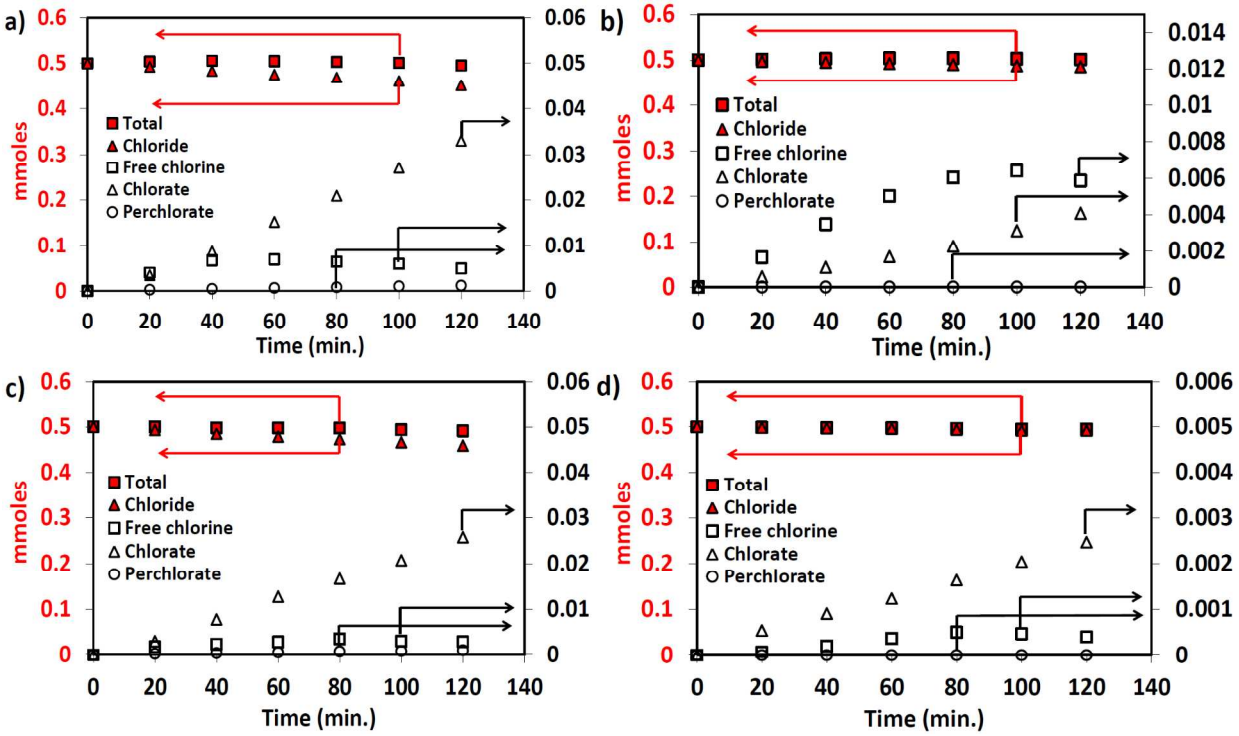

Figure S4. Duplicate experiment to that shown in the main manuscript. Total, free chlorine, chlorate, perchlorate, and chlorine mole balance for a) BDD-O without phenol; b) BDDF-aliphatic without phenol; c) BDD-O with phenol; and d) BDDF-aliphatic with phenol.

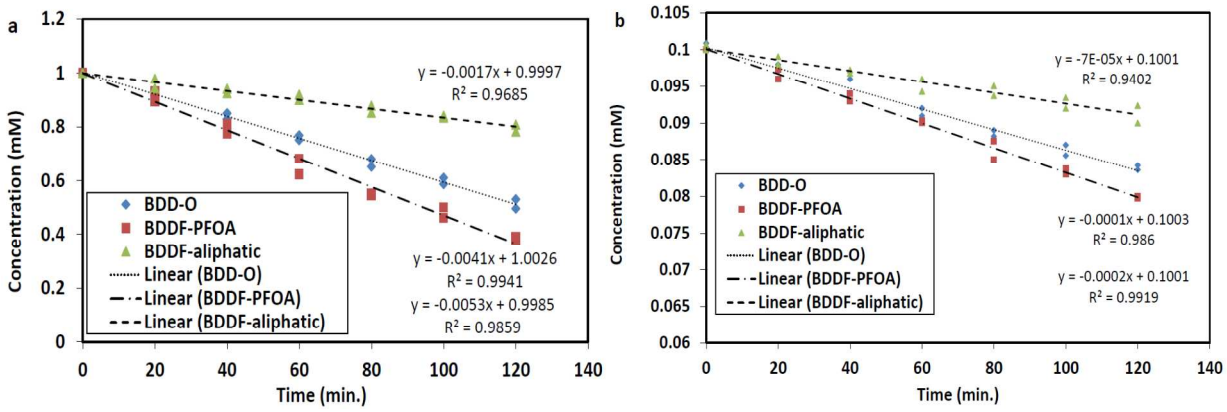

Figure S5. Bulk oxidation of a) 1mM phenol and b) 0.1mM TA for BDD-O, BDDF-PFOA and BDDF-aliphatic at 22^0C.

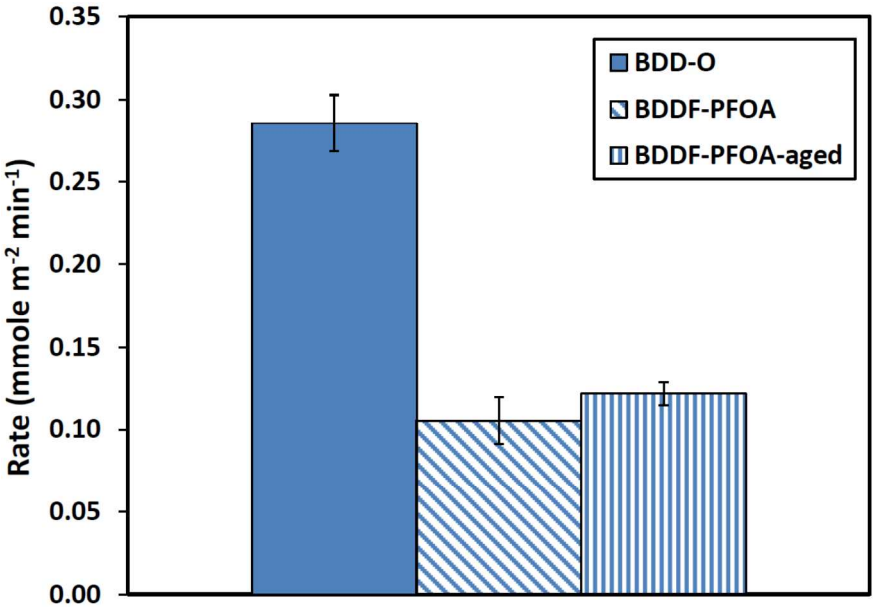

Figure S6. Perchlorate formation rates for BDD-O, BDDF-PFOA & BDDF-PFOA-aged.

6.0 References

1. Bard, A. J.; Faulkner, L. R. *Fundamentals and Applications: Electrochemical Methods,* 2nd ed.; Wiley: New York, 2001.
2. Loh, W.; Tonegutti, C. A.; Volpe, P. L. O. Diffusion Coefficients of Aqueous Phenols Determined by the Taylor Dispersion Technique. Evidence for Solute Adsorption on the Walls of Teflon Tubing. *J. Chem. Soc., Faraday Trans.* **1993**, 89.1, 113-118.
3. Papaspyrides, C. D.; Vouyiouka, S. N. *Solid State Polymerization*; Wiley: New Jersey, 2009.